Published in final edited form as:
Cephalalgia. 2012 March ; 32(4): 279–288. doi:10.1177/0333102411435985.

Cerebral perfusion changes in migraineurs: a voxelwise comparison of interictal dynamic susceptibility contrast MRI measurements

Enrico B Arkink, MD[1,*], **Egbert JW Bleeker**[1,3,*], **Nicole Schmitz, PhD**[1], **Guus G Schoonman, MD, PhD**[2], **Ona Wu, PhD**[4], **Michel D Ferrari, MD, PhD**[2], **Mark A van Buchem, MD, PhD**[1,3], **Matthias JP van Osch, PhD**[1,3], and **Mark C Kruit, MD, PhD**[1]

[1]Department of Radiology, Leiden University Medical Center, Leiden, the Netherlands [2]Department of Neurology, Leiden University Medical Center, Leiden, the Netherlands [3]C.J. Gorter Center for High Field MRI, Leiden, The Netherlands [4]Martinos Center, Massachusetts General Hospital, Boston, Massachusetts, USA

Abstract

Introduction—The increased risk of cerebro- and cardiovascular disease in migraineurs may be the consequence of a systemic condition affecting whole body vasculature. At cerebrovascular level, this may be reflected by interictal global or regional cerebral perfusion abnormalities. Whether focal perfusion changes occur during interictal migraine has not been convincingly demonstrated.

Methods—We measured brain perfusion with dynamic susceptibility contrast magnetic resonance imaging (DSC-MRI) in 29 interictal female migraineurs (12 migraine with aura (MA), 17 migraine without aura (MO)) and 16 female controls. Perfusion maps were compared between these groups with a voxelwise ($p<0.001$, uncorrected, minimum cluster size 20 voxels) and a region-of-interest approach.

Results—In whole brain voxelwise analyses interictal hyperperfusion was observed in the left medial frontal gyrus in migraineurs and in the inferior and middle temporal gyrus in MO patients, in comparison to controls. Hypoperfusion was seen in the postcentral gyrus and in the inferior temporal gyrus in MA patients and in the inferior frontal gyrus in MO patients. Additional focal sites of hyperperfusion were noted in subgroups based on attack frequency and disease history. Region-of-interest analyses of the pons, hypothalamus, occipital lobe and cerebellum did not show interictal perfusion differences between migraineurs and controls.

Conclusion—We conclude that interictal migraine is characterized by discrete areas of hyper- and hypoperfusion unspecific for migraine pathophysiology and not explaining the increased vulnerability of particular brain regions for cerebrovascular damage.

Address for correspondence:: E.B. Arkink, MD, Department of Radiology, Leiden University Medical Center, PO Box 9600, 2300 RC, Leiden, the Netherlands. Tel + 31 71 526 3681, fax + 31 71 524 8256, e.b.arkink@lumc.nl.
*First two authors contributed equally to this work

Declaration of conflicting interests
Ona Wu has a patent on "Delay-compensated calculation of tissue blood flow," US Patent 7,512,435. March 31, 2009, and the patent has been licensed to General E, Siemens, and Olea Medical. The remaining authors declare that there is no conflict of interest regarding the subject matter of this article.

Keywords

interictal migraine; dynamic susceptibility contrast magnetic resonance imaging; brain perfusion

Introduction

Migraine is a prevalent neurovascular disorder, characterized by recurrent attacks of disabling headache accompanied by dysfunction of the autonomic nervous system. In up to a third of the patients, neurological (mostly visual) aura symptoms precede or accompany the headache phase of migraine attacks (1). Migraine, especially migraine with aura (MA), has been identified as an independent risk factor for clinical and subclinical brain infarction. (2;3) The posterior circulation territory, notably the cerebellum, seems to be specifically vulnerable.(2;4;5) Further, female migraineurs both with and without aura are at increased risk of deep white matter and brainstem hyperintensities (2;5;6). Repetitive physiological and biochemical changes during migraine attacks, including changes in brain perfusion, are amongst the mechanisms proposed to explain or contribute to the increased risk of ischemic brain lesions (7).

Besides the increased risk of cerebrovascular complications in migraineurs, there is increasing evidence that migraine is also independently associated with other (ischemic) vascular disorders, including angina pectoris, myocardial infarction, claudication and retinopathy (7;8). Since it is unlikely that these conditions are all direct consequences of migraine attacks, or that they induce migraine themselves, a more plausible interpretation of these associations is that both migraine and these vascular disorders are influenced by subtle systemic changes in the vessel wall and its interaction with circulating coagulation factors, platelets and other substances. The diversity of organs involved suggests a systemic condition to play a role in the pathogenesis of these conditions. Several observations in migraineurs support this concept, including interictal evidence of endothelium (dependent) dysfunction, impaired cerebrovascular reactivity, reports on ictal and interictal generalized or coronary artery vasospasm, impaired brachial artery compliance, increased aortic stiffness and hypercoagulability, which all seem to be independent of the coincidence of established cardiovascular risk factors (9).

Since several of the observed systemic changes in migraineurs are persistent threats, and since they could result in changes in brain perfusion, detection of changes in brain perfusion in migraineurs could be expected interictally. Earlier single photon emission computed tomography (SPECT) reported gross differences in cerebral hemodynamics between interictal migraineurs and control subjects, but results were contradictory (10–15). More recent perfusion studies, using positron emission tomography (PET) (16–20) and dynamic susceptibility contrast magnetic resonance imaging (DSC-MRI) (21–24), concentrated on the ictal phenomena, so it has still not been convincingly proven whether in the interictal stage of migraine, differences in cerebral hemodynamics are present or absent in comparison with headache-free control subjects.

In the current study, we investigated interictal groups of MA and migraine without aura (MO) patients and controls, using DSC-MRI. DSC-MRI has several advantages compared to earlier performed PET and SPECT studies, including a better spatial resolution with whole-brain coverage and a higher signal-to-noise ratio (SNR), allowing for voxelwise detection of small perfusion differences (25). We performed unbiased whole brain voxelwise analyses of cerebral blood flow (CBF), cerebral blood volume (CBV), mean transit time (MTT) and time-to-peak (TTP) maps, but also performed region-of-interest analyses in predefined regions that have been reported to show perfusion changes during the different stages of

migraine, or that have been reported to be specifically at risk for ischemic lesion development, such as the cerebellum.

Methods

Subject population

Thirty female migraine patients (13 MA: mean age 42.9, range 28–52; 17 MO: mean age 47.6, range 38–57) and seventeen female control subjects (mean age 39.9, range 21–55) participated in this study. Migraine patients were enrolled through advertisements in newspapers and magazines. Migraineurs were diagnosed with MA or MO according to the criteria of the Headache Classification Committee of the International Headache Society (IHS) (1) at the Department of Neurology (GGS); headache-free, unrelated control subjects without a history of migraine attacks or other headaches were recruited by local advertisement and enrolled in the study. A total of 25 migraine patients were able to estimate their average number of attacks and/or duration of headache. None of the migraine patients were taking prophylactic medication. All were headache-free for at least 7 days before and 2 days after the MRI examination (verified by telephonic consultation). The study was approved by the institutional review board and all subjects gave written and informed consent.

Neuroimaging protocol

T_2-weighted turbo spin echo images (repetition time (TR)/ echo time (TE) 4741/80 ms, echo train length 16, acquisition matrix 448×392 mm, FOV 224×180 mm^2, 48 slices of 3 mm thickness) and fluid-attenuated inversion recovery (FLAIR) (TR/TE 10128/120 ms, echo train length 36, acquisition matrix 224×224, FOV 224×180 mm^2, 48 slices of 3 mm thickness) were acquired on a 3.0 Tesla MRI system (Achieva, Philips Medical Systems, Best, The Netherlands) and evaluated by an experienced neuroradiologist (MCK). Two cases showing structural brain abnormalities that could have impeded or confounded perfusion image post processing were excluded from further analyses: one control subject with a frontal cortical infarct, and one MA patient with confluent white matter hyperintensities (WMHs). Small, punctuate deep WMHs were not considered an exclusion criterion.

DSC-MR imaging was performed using an 8-channel receive array head coil; 0.2 ml/kg-bodyweight Gd-DTPA (Magnevist®, Schering) was injected intravenously at 5 ml/sec followed by a saline chaser of 25 ml (injected at 5 ml/s (20 ml) and 2 ml/s (5 ml)). PRESTO (PRinciples of Echo-Shifting with a Train of Observations, a 3D ultrafast gradient echo sequence combining whole brain coverage with T_2*-weighted imaging (26)) was used for the acquisition with the following parameters: data matrix 64×53 mm (zerofilled to 128×108 mm), TE/TR 26/17 ms, flip angle 5°, field of view (FOV) 224×168 mm^2, SENSE factor of 2.4, 48 slices of 3 mm thickness, number of echoes in a echo train 21, and 60 segments per volume resulting in a dynamic scan time of 1.1 sec.

Post-processing

The perfusion maps of CBF, CBV, MTT and TTP were generated using software developed at the Massachusetts General Hospital using block-circulant singular value decomposition with oscillation index regularization (27). This program requires a manual selection of the arterial input function (AIF, the passage of contrast agent through a major brain-feeding artery). At least eight voxels near the middle cerebral artery were selected to form the global AIF used in the deconvolution.

The signal drop in the T_2*-weighted images resulting from the contrast agent passage was converted to the concentration contrast agent (C(t)) using

$$C(t) \sim \Delta R_2^* = -\frac{1}{TE} \log\left(\frac{S(t)}{S(0)}\right) \quad [1]$$

The deconvolution was performed over the first and second passage of the gadolinium concentration passage with a noise threshold of 0.4 and an oscillation threshold of 0.095.

The CBF maps were used to determine the transformation parameters for coregistration of all perfusion maps spatially to the PET template in SPM5 (Wellcome Trust Centre for Neuroimaging, Institute of Neurology, UCL, London UK – http://www.fil.ion.ucl.ac.uk/spm). To improve the spatial normalization further, an average CBF map was constructed over all subjects and the individual CBF maps were coregistered to that average CBF template together with all other perfusion maps. The relative CBF and relative CBV maps were converted to quantitative CBF and CBV maps by setting the white matter CBF to 22 ml/100g/min (28). The white matter segmentation for this quantification step was performed in SPM5 on the CBF map; the segmentation mask consisted of all voxels with a 95% or higher certainty that the voxel is white matter.

Statistical analyses

All perfusion maps were smoothed using an isotropic Gaussian kernel (full width at half maximum of 8 mm). Whole brain voxelwise comparison was performed, comparing interictal scans of MA, MO and control subjects using one-way analyses of variance implemented in SPM5, correcting for age. Further subanalyses, also corrected for age, were performed comparing controls to migraineurs with a high (HF, > 2 attacks/month, n=12) and a low (LF, ≤2 attacks/month, n=13) attack frequency and to migraineurs with a long (LH, > median of 28 years) and a short (SH, ≤28 years) disease duration. For statistical tests, the probability threshold was set at $p<0.001$, uncorrected for multiple comparisons, with a cluster extent of minimal 20 neighboring voxels.

Next to voxel-based comparison, regions-of-interest (ROIs) for the occipital lobe and cerebellum (constructed from the corresponding regions from the automated anatomical labeling (AAL) template for SPM5) (29), the pons and the hypothalamus (drawn manually and incorporated into the AAL template) were created to study the average distribution of perfusion parameters in these areas in the normalized, non-smoothed images. The choice of ROIs for pons, hypothalamus and occipital lobe was based on previous reports of hemodynamic changes during migraine (16;18–20). The cerebellum was analyzed specifically because of its suggested increased vulnerability for cerebellar infarction in migraineurs. Distributions of mean CBF, CBV, MTT and TTP were compared between migraine patients and control subjects using multivariate general linear models adjusted for age in SPSS for Windows, release 16.0.2 (Chicago, USA). Subanalyses were carried out to investigate the influence of disease history and attack frequency on these hemodynamic parameters.

Results

After exclusion of the two participants with larger brain abnormalities, 45 female subjects remained for analysis: 12 MA patients, 17 MO patients, and 16 control subjects for further analysis. Mean age (MA 42.9±8.2 years, MO 47.6±5.3 years, controls 39.9±12.3, $p>0.05$, one-way ANOVA) was not different across the groups. Migraineurs had a mean of 3.1±2.2 attacks per month and a history of migraine of 28±11 years.

The results of the voxelwise whole brain comparison between interictal migraineurs and controls are shown in Table 1 and Figures 1 and 2. We found a higher CBF in a part of the left medial frontal gyrus when analyzing the whole group of migraineurs vs. controls (Figure 1A). This difference remained, also when assessing MA and MO groups separately vs. controls (not shown in figure). CBF was also increased in the right inferior gyrus in MO (Fig 1B). Decreased CBF was observed in parts of the right inferior temporal gyrus (Fig. 1C) and the left postcentral gyrus (Fig. 1D) in MA patients and in part of the inferior frontal gyrus in MO patients (Fig. 1E). CBV was increased in part of the right inferior and middle temporal gyrus in MO (Figure 2). CBV reductions were not identified. In addition, no increases or decreases in MTT and TTP were observed between migraineurs and control subjects.

In voxelwise subanalyses effects of attack frequency and disease duration were assessed (Tables 2 and 3). This revealed areas in the left medial frontal gyrus of higher local CBF in HF migraineurs, and lower CBF in LF migraineurs when compared to controls. Further there were several other areas of increased local CBF when HF migraineurs were contrasted to LF migraineurs. Analyses based on disease duration revealed a mixture of CBF findings for SH and LH migraineurs. Areas of increased CBV and MTT were uniquely identified in SH migraineurs, either contrasted to controls or to LH migraineurs.

The ROI-analyses of CBF, CBV, MTT and TTP in pons, hypothalamus, occipital lobe and cerebellum showed no differences between migraineurs and controls, nor between migraine subgroups and controls (Supplementary table 1).

Discussion

To the best of our knowledge, this is the first explorative DSC-MRI study assessing brain perfusion characteristics and patterns in female migraine patients in an interictal state vs. headache-free control subjects. In this relatively large sample of migraineurs (MA and MO) and control subjects, our voxelwise comparison of perfusion maps identified some small areas of perfusion differences between migraineurs and controls, including both hyper- and hypoperfusion in frontal, parietal, and temporal regions in the interictal migraine brain. Similarly, a variety of additional areas of perfusion differences appeared in voxelwise subanalyses based on attack frequency and disease duration, including several focal areas in the frontal and parietal lobes, the putamen and the cerebellum. In these data, a predominance seems to exist for areas with higher CBF values in migraineurs with higher attack frequencies, and for areas with lower CBV and MTT values in migraineurs with shorter disease history. Analyses assessing regional perfusion differences in the pons, hypothalamus, occipital lobe and cerebellum between (subgroups) of interictal migraineurs and controls did not show significant differences.

Areas with altered interictal perfusion may reflect local interictal differences in neuronal (metabolic) activity or density. This could be the consequence of repetitive migraine attacks or chronic adapative mechanisms, leading to neuroplastic changes in cortical and subcortical structures. Other explanations include the presence of some degree of interictal cerebrovascular dysregulation in migraineurs, or a (migraine disease-related) systemic condition altering vessel wall characteristics that impede normal regional blood flow. The findings in the subgroups with higher attack frequency and shorter migraine duration may relate to any of these potential mechanisms, although we were not able to access the direction of such potential associations. One could speculate that periods of hypoperfusion reflect periods of transient ischemia, that are followed by periods of hyperperfusion to compensate for deficits that have developed in the meantime. Concurrent vasodilatation may explain increases in CBV equally to those in CBF, leaving MTT and TTP unaltered. If no

vasodilatation occurs, an increase in CBV may be accompanied by an increase in MTT, like seen in some of the focal areas of hyperperfusion in SH migraineurs.

Most if not all currently identified areas of altered perfusion have earlier been somehow reported in structural imaging studies in migraine or other pain conditions. For instance, the area of higher CBF that we identified in the left medial frontal gyrus, seems to co-localize with a reported area of gray matter reductions in migraine patients (30). Gray matter changes in the medial frontal gyrus have been reported to correlate with pain scores in another chronic pain condition, fibromyalgia (31), suggesting a correlation between morphology and function. Similarly, it is tempting to correlate our findings in HF migraine patients of increased CBF in the postcentral gyrus to thickening of the somatosensory cortex in migraineurs, that was described in one earlier morphometric study, and that was suggested to be an adaptation to repetitive migraine attacks (32).

Although thus seemingly altered interictal perfusion in certain brain areas in migraineurs might be co-localized with earlier reported structural or hemodynamic changes in the brains of patients with migraine and other pain conditions, we want to stress that the changes measured by DSC-MRI are small, a direct correlation between functional and structural changes is still lacking, and the nature of any of such potential associations remains unclear and difficult to interpret. For instance, higher or lower perfusion did not consistently relate to specific structural changes: hypoperfusion seems in some areas to be related with reported cortical thickening, and in other areas with described gray matter reduction. The interpretation of the hemodynamic differences is further hampered by the lack of a histopathologic correlate for the described structural changes in migraine brains: gray matter volume or “density” on MRI scans is influenced by neuron number and size, the amount of extracellular or microvascular fluid, gliosis and atrophy. In this matter, we should also consider that cell density is not necessarily directly related to the neuronal metabolic activity. Future studies may overcome some of these major interpretative limitations of our study by directly comparing (voxelwise) structural imaging measures with (voxelwise) perfusion imaging approaches.

We found no interictal differences in CBF, CBV, MTT or TTP in the regional maps of the pons, hypothalamus and occipital lobe, although perfusion changes have previously been identified in these areas during migraine attacks (16;18–20;22). Similarly, we found no interictal perfusion abnormalities in the cerebellum in the total group of migraineurs. These negative interictal findings may be explained e.g. by high inter- and intra-individual variance in cerebral hemodynamics, and of course do not exclude the possibility of ictal perfusion changes in these areas. In the voxelwise analyses, we found however focal increases in CBV in the cerebellum of SH migraineurs, accompanied by a longer MTT in the same area, compared to both controls and LH migraineurs. Further studies should assess whether these perfusion changes may relate to the known increased vulnerability of the cerebellum to infarction.

All migraineurs in our study were scanned at least seven days after the last migraine attack and none of them suffered their next attack within two days after scanning. Inter-individual variance in hemodynamics may however still have been influenced by the specific moment in the migraine cycle in which each individual subject has been examined; we regard this as a hard to overcome limitation of our study. Future studies should assess the reproducibility of and/or variation in regional cerebral perfusion changes during different (interictal and ictal) timepoints in the migraine cycle.

We are not aware of any PET or DSC-MRI studies that report perfusion differences in migraineurs during interictal stage in comparison with control subjects. There are however

several reports on interictal CBF changes in regular migraine compared to controls, measured with SPECT, but results are contradicting. Lauritzen et al. did not find interictal CBF changes when comparing 11 migraineurs to 20 controls (14). Levine et al. reported general hypoperfusion in 15 MA and 12 MO patients in the posterior circulation territory, compared to 20 controls (15). Other studies reported single or multiple foci of interictal hypoperfusion in 43–67% of migraineurs (10;11). However, yet another SPECT study reported interictal global *hyper*perfusion in 50 MO patients (mainly located in frontal regions) and global *hypo*perfusion in 20 MA patients (mainly located in posterior regions), compared to control subjects (12). These contradicting results may be due to the unreliability of visual evaluation of SPECT-derived CBF images in terms of picking up abnormalities in interictal migraineurs (13). The small focal areas of hyper- and hypoperfusion we observed in frontal, temporal, and parietal regions in migraine patients compared to controls seem to show overlap with some of the regions found in the aforementioned SPECT studies, but comparison between these different techniques remains complicated because of differences in post-processing, which is discussed further below.

Up till now, DSC-MRI has been performed in only a few occasions in regular migraine with and without aura (21–24); DSC-MRI has most often been used for studying perfusion changes during attacks of rare subtypes of migraine, such as familial hemiplegic migraine or persistent migraine aura, most often only in a single case (33–40). The DSC-MRI acquisition and analysis in the current study was applied with more advanced acquisition and post-processing techniques than previously used in DSC-MRI studies in regular migraine (24). First, the 3D PRESTO acquisition in combination with parallel imaging covered the entire brain at a temporal resolution of 1.1 seconds. A low dynamic scan time is important because the concentration contrast agent is monitored dynamically, and a simulation study by Knutsson et al. showed that the dynamic scan time should be below 1.5 secs (41). Second, delay-insensitive deconvolution was used. This improves the quality of the perfusion estimates, especially since delay effects are more present when a global AIF is used for the deconvolution (42;43). In our analysis, a global AIF was selected close but outside the middle cerebral arteries (44). These two brain-feeding arteries supply the majority of but not the entire cortex. Third, spatial normalization was performed in two steps, first to the PET template and second to an average CBF map. This improves the accuracy of the voxelwise comparison analysis. Apart from an increased spatial resolution allowing for voxelwise comparisons, DSC-MRI has several advantages compared to other techniques used for measuring perfusion in migraine. DSC-MRI does not expose the subjects to ionizing radiation and is therefore better suited for measuring cerebral perfusion in large samples of both migraineurs as well as controls than PET or SPECT. Further, DSC-MRI is more widely available and less time consuming. SPECT only measures CBF and some SPECT techniques provide only relative values. Furthermore, the spatial resolution of PET and SPECT is lower than of DSC-MRI making it harder to detect local perfusion changes. In the SPECT studies that compared interictal migraineurs to controls, images were acquired with varying SPECT-contrast agents and were often evaluated visually or analysed semiquantitatively leading to a substantial degree of subjectivity. To overcome this problem, our results of local hyper- and hypoperfused areas between migraine attacks were generated by an unbiased whole brain voxelwise comparison of DSC-MRI images. Besides aforementioned advantages, DSC-MRI also has a major disadvantage. Recent studies showed that the (repetitive) use of DSC-MRI contrast agents in patients with renal failure increases the risk for attaining nephrogenic systemic fibrosis (NSF) (45;46), although this seems to be limited to certain specific agents. Arterial spin-labeling (ASL) likely is a good alternative technique for both DSC-MRI and PET. ASL, a relatively new MR technique, is better for perfusion estimation and has the possibility for repeated measurements to increase the sensitivity (47). Although this technique only allows for absolute quantification of CBF (and not CBV or MTT), intravenous administration of contrast agents or radioactive tracers

is not necessary. The first results of ASL during migraine attacks show results comparable to those in PET studies (48;49).

In summary, our study shows in an unbiased whole brain voxelwise approach that interictal migraineurs have discrete areas of cerebral hyper- and hypoperfusion, measured with DSC-MRI. Their specificity for migraine pathophysiology is thought to be small, and we did not find changes in hemodynamics of interictal migraineurs that likely account for subclinical cerebellar lesions found previously.

Supplementary Material

Refer to Web version on PubMed Central for supplementary material.

Acknowledgments

Funding acknowledgement

This work was supported by the Dutch Brain Foundation (Nederlandse Hersenstichting, HsN H04/08) and the Dutch Technology Foundation (STW VENI 7291) and in part by grant R01 NS059775 (OW) from the National Institutes of Health.

Reference List

1. Headache Classification Subcommittee of the International Headache Society. The International Classification of Headache Disorders. Cephalalgia (2nd edition). 2004; 24(Suppl 1):9–160. [PubMed: 14979299]
2. Kruit MC, van Buchem MA, Hofman PA, Bakkers JT, Terwindt GM, Ferrari MD, et al. Migraine as a risk factor for subclinical brain lesions. JAMA. 2004; 291:427–434. [PubMed: 14747499]
3. Schürks M, Rist PM, Bigal ME, Buring JE, Lipton RB, Kurth T. Migraine and cardiovascular disease: systematic review and meta-analysis. BMJ. 2009; 339:b3914. [PubMed: 19861375]
4. Kruit MC, Launer LJ, Ferrari MD, van Buchem MA. Infarcts in the posterior circulation territory in migraine. The population-based MRI CAMERA study. Brain. 2005; 128:2068–2077. [PubMed: 16006538]
5. Scher AI, Gudmundsson LS, Sigurdsson S, Ghambaryan A, Aspelund T, Eiriksdottir G, et al. Migraine headache in middle age and late-life brain infarcts. JAMA. 2009; 301:2563–2570. [PubMed: 19549973]
6. Kruit MC, Launer LJ, Ferrari MD, van Buchem MA. Brain stem and cerebellar hyperintense lesions in migraine. Stroke. 2006; 37:1109–1112. [PubMed: 16497982]
7. Bigal ME, Kurth T, Hu H, Santanello N, Lipton RB. Migraine and cardiovascular disease: possible mechanisms of interaction. Neurology. 2009; 72:1864–1871. [PubMed: 19470970]
8. Bigal ME, Kurth T, Santanello N, Buse D, Golden W, Robbins M, et al. Migraine and cardiovascular disease: a population-based study. Neurology. 2010; 74:628–635. [PubMed: 20147658]
9. Tietjen GE. Migraine as a systemic vasculopathy. Cephalalgia. 2009; 29:987–996. [PubMed: 19689607]
10. Calandre EP, Bembibre J, Arnedo ML, Becerra D. Cognitive disturbances and regional cerebral blood flow abnormalities in migraine patients: their relationship with the clinical manifestations of the illness. Cephalalgia. 2002; 22:291–302. [PubMed: 12100092]
11. De Benedittis G, Ferrari Da Passano C, Granata G, Lorenzetti A. CBF changes during headache-free periods and spontaneous/induced attacks in migraine with and without aura: a TCD and SPECT comparison study. J Neurosurg Sci. 1999; 43:141–146. [PubMed: 10735768]
12. Facco E, Munari M, Baratto F, Behr AU, Dal Palu A, Cesaro S, et al. Regional cerebral blood flow (rCBF) in migraine during the interictal period: different rCBF patterns in patients with and without aura. Cephalalgia. 1996; 16:161–168. [PubMed: 8734767]

13. Friberg L, Olesen J, Iversen H, Nicolic I, Sperling B, Lassen NA, et al. Interictal 'patchy' regional cerebral blood flow patterns in migraine patients. A single photon emission computerized tomographic study. Eur J Neurol. 1994; 1:35–43.
14. Lauritzen M, Olesen J. Regional cerebral blood flow during migraine attacks by Xenon-133 inhalation and emission tomography. Brain. 1984; 107((Pt 2)):447–461. [PubMed: 6609739]
15. Levine SR, Welch KM, Ewing JR, Robertson WM. Asymmetric cerebral blood flow patterns in migraine. Cephalalgia. 1987; 7:245–248. [PubMed: 3427624]
16. Afridi SK, Giffin NJ, Kaube H, Friston KJ, Ward NS, Frackowiak RS, et al. A positron emission tomographic study in spontaneous migraine. Arch Neurol. 2005; 62:1270–1275. [PubMed: 16087768]
17. Bahra A, Matharu MS, Buchel C, Frackowiak RS, Goadsby PJ. Brainstem activation specific to migraine headache. Lancet. 2001; 357:1016–1017. [PubMed: 11293599]
18. Denuelle M, Fabre N, Payoux P, Chollet F, Geraud G. Hypothalamic activation in spontaneous migraine attacks. Headache. 2007; 47:1418–1426. [PubMed: 18052951]
19. Denuelle M, Fabre N, Payoux P, Chollet F, Geraud G. Posterior cerebral hypoperfusion in migraine without aura. Cephalalgia. 2008; 28:856–862. [PubMed: 18513260]
20. Weiller C, May A, Limmroth V, Juptner M, Kaube H, Schayck RV, et al. Brain stem activation in spontaneous human migraine attacks. Nat Med. 1995; 1:658–660. [PubMed: 7585147]
21. Cutrer FM, Sorensen AG, Weisskoff RM, Østergaard L, Sanchez del Rio M, Lee EJ, et al. Perfusion-weighted imaging defects during spontaneous migrainous aura. Ann Neurol. 1998; 43:25–31. [PubMed: 9450765]
22. Kapinos G, Fischbein NJ, Zaharchuk G, Venkatasubramanian C. Migraine-like headache with visual deficit and perfusion abnormality on MRI. Neurology. 2010; 74:1743–1745. [PubMed: 20498443]
23. Linn J, Freilinger T, Morhard D, Bruckmann H, Straube A. Aphasic migraineous aura with left parietal hypoperfusion: a case report. Cephalalgia. 2007; 27:850–853. [PubMed: 17598767]
24. Sanchez del Rio M, Bakker D, Wu O, Agosti R, Mitsikostas DD, Østergaard L, et al. Perfusion weighted imaging during migraine: spontaneous visual aura and headache. Cephalalgia. 1999; 19:701–707. [PubMed: 10570723]
25. Cavallin L, Axelsson R, Wahlund LO, Oksengard AR, Svensson L, Juhlin P, et al. Voxel-based correlation between coregistered single-photon emission computed tomography and dynamic susceptibility contrast magnetic resonance imaging in subjects with suspected Alzheimer disease. Acta Radiol. 2008; 49:1154–1161. [PubMed: 18855165]
26. Liu G, Sobering G, Duyn J, Moonen CT. A functional MRI technique combining principles of echo-shifting with a train of observations (PRESTO). Magn Reson Med. 1993; 30:764–768. [PubMed: 8139461]
27. Wu O, Østergaard L, Weisskoff RM, Benner T, Rosen BR, Sorensen AG. Tracer arrival timing-insensitive technique for estimating flow in MR perfusion-weighted imaging using singular value decomposition with a block-circulant deconvolution matrix. Magn Reson Med. 2003; 50:164–174. [PubMed: 12815691]
28. Østergaard L, Sorensen AG, Kwong KK, Weisskoff RM, Gyldensted C, Rosen BR. High resolution measurement of cerebral blood flow using intravascular tracer bolus passages. Part II: Experimental comparison and preliminary results. Magn Reson Med. 1996; 36:726–736. [PubMed: 8916023]
29. Tzourio-Mazoyer N, Landeau B, Papathanassiou D, Crivello F, Etard O, Delcroix N, et al. Automated anatomical labeling of activations in SPM using a macroscopic anatomical parcellation of the MNI MRI single-subject brain. Neuroimage. 2002; 15:273–289. [PubMed: 11771995]
30. Kim JH, Suh SI, Seol HY, Oh K, Seo WK, Yu SW, et al. Regional grey matter changes in patients with migraine: a voxel-based morphometry study. Cephalalgia. 2008; 28:598–604. [PubMed: 18422725]
31. Luerding R, Weigand T, Bogdahn U, Schmidt-Wilcke T. Working memory performance is correlated with local brain morphology in the medial frontal and anterior cingulate cortex in fibromyalgia patients: structural correlates of pain-cognition interaction. Brain. 2008; 131:3222–3231. [PubMed: 18819988]

32. DaSilva AF, Granziera C, Snyder J, Hadjikhani N. Thickening in the somatosensory cortex of patients with migraine. Neurology. 2007; 69:1990–1995. [PubMed: 18025393]
33. Hsu DA, Stafstrom CE, Rowley HA, Kiff JE, Dulli DA. Hemiplegic migraine: hyperperfusion and abortive therapy with intravenous verapamil. Brain Dev. 2008; 30:86–90. [PubMed: 17614229]
34. Jacob A, Mahavish K, Bowden A, Smith ET, Enevoldson P, White RP. Imaging abnormalities in sporadic hemiplegic migraine on conventional MRI, diffusion and perfusion MRI and MRS. Cephalalgia. 2006; 26:1004–1009. [PubMed: 16886937]
35. Jäger HR, Giffin NJ, Goadsby PJ. Diffusion- and perfusion-weighted MR imaging in persistent migrainous visual disturbances. Cephalalgia. 2005; 25:323–332. [PubMed: 15839846]
36. Lindahl AJ, Allder S, Jefferson D, Allder S, Moody A, Martel A. Prolonged hemiplegic migraine associated with unilateral hyperperfusion on perfusion weighted magnetic resonance imaging. J Neurol Neurosurg Psychiatry. 2002; 73:202–203. [PubMed: 12122185]
37. Masuzaki M, Utsunomiya H, Yasumoto S, Mitsudome A. A case of hemiplegic migraine in childhood: transient unilateral hyperperfusion revealed by perfusion MR imaging and MR angiography. AJNR Am J Neuroradiol. 2001; 22:1795–1797. [PubMed: 11673182]
38. Oberndorfer S, Wober C, Nasel C, Asenbaum S, Lahrmann H, Fueger B, et al. Familial hemiplegic migraine: follow-up findings of diffusion-weighted magnetic resonance imaging (MRI), perfusion-MRI and [99mTc] HMPAO-SPECT in a patient with prolonged hemiplegic aura. Cephalalgia. 2004; 24:533–539. [PubMed: 15196295]
39. Relja G, Granato A, Ukmar M, Ferretti G, Antonello RM, Zorzon M. Persistent aura without infarction: decription of the first case studied with both brain SPECT and perfusion MRI. Cephalalgia. 2005; 25:56–59. [PubMed: 15606571]
40. San-Juan OD, Zermeno PF. Migraine with persistent aura in a Mexican patient: case report and review of the literature. Cephalalgia. 2007; 27:456–460. [PubMed: 17388804]
41. Knutsson L, Stahlberg F, Wirestam R. Aspects on the accuracy of cerebral perfusion parameters obtained by dynamic susceptibility contrast MRI: a simulation study. Magn Reson Imaging. 2004; 22:789–798. [PubMed: 15234447]
42. Calamante F, Gadian DG, Connelly A. Delay and dispersion effects in dynamic susceptibility contrast MRI: simulations using singular value decomposition. Magn Reson Med. 2000; 44:466–473. [PubMed: 10975900]
43. Wu O, Østergaard L, Koroshetz WJ, Schwamm LH, O'Donnell J, Schaefer PW, et al. Effects of tracer arrival time on flow estimates in MR perfusion-weighted imaging. Magn Reson Med. 2003; 50:856–864. [PubMed: 14523973]
44. Bleeker EJ, van Buchem MA, van Osch MJ. Optimal location for arterial input function measurements near the middle cerebral artery in first-pass perfusion MRI. J Cereb Blood Flow Metab. 2009; 29:840–852. [PubMed: 19142193]
45. Idée JM, Port M, Medina C, Lancelot E, Fayoux E, Ballet S, et al. Possible involvement of gadolinium chelates in the pathophysiology of nephrogenic systemic fibrosis: a critical review. Toxicology. 2008; 248:77–88. [PubMed: 18440117]
46. Thomsen HS, Marckmann P, Logager VB. Update on nephrogenic systemic fibrosis. Magn Reson Imaging Clin N Am. 2008; 16:551–560. vii. [PubMed: 18926421]
47. Williams DS, Detre JA, Leigh JS, Koretsky AP. Magnetic resonance imaging of perfusion using spin inversion of arterial water. Proc Natl Acad Sci U S A. 1992; 89:212–216. [PubMed: 1729691]
48. Kato Y, Araki N, Matsuda H, Ito Y, Suzuki C. Arterial spin-labeled MRI study of migraine attacks treated with rizatriptan. J Headache Pain. 2010; 11:255–258. [PubMed: 20411294]
49. Pollock JM, Deibler AR, Burdette JH, Kraft RA, Tan H, Evans AB, et al. Migraine associated cerebral hyperperfusion with arterial spin-labeled MR imaging. AJNR Am J Neuroradiol. 2008; 29:1494–1497. [PubMed: 18499796]

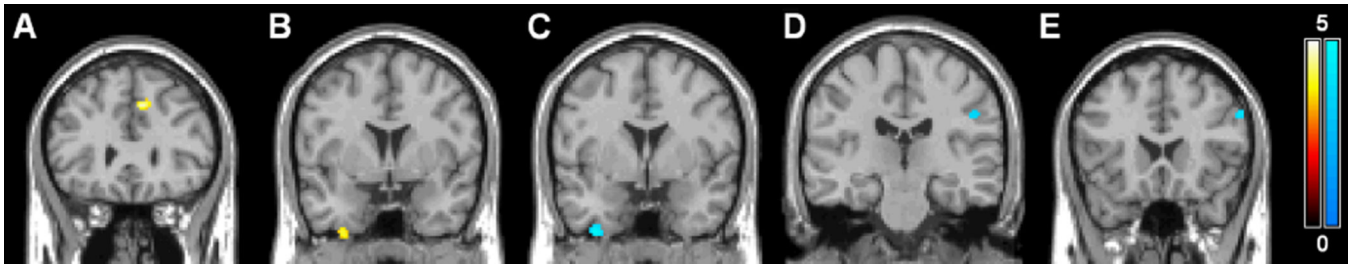

Figure 1.

Statistical parametric maps demonstrating increases (yellow) and decreases (blue) in DSC-MRI measured cerebral blood flow (CBF). Increases in CBF between migraineurs and controls in the medial frontal gyrus (A) and between MO patients and controls in the inferior temporal gyrus (B) and decreases in CBF between MA patients and controls in the inferior temporal gyrus (C) and postcentral gyrus (D) and between MO patients and controls in the inferior frontal gyrus (E) are superimposed on a single subject T1 template coregistered to the standard SPM5 PET template. Color bars represent Z-values. The left side of each picture is the right side of the brain.

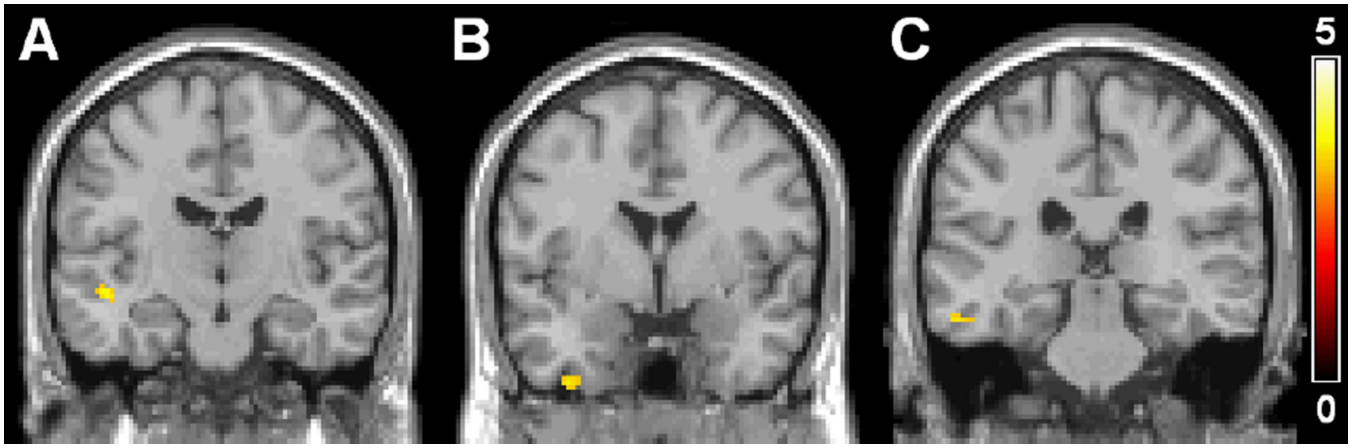

Figure 2.

Statistical parametric maps demonstrating increases in DSC-MRI measured cerebral blood volume (CBV) in MO patients compared to headache-free control subjects in the middle temporal gyrus (A) and inferior temporal gyrus (B, C), superimposed on the single subject T1 template coregistered to the standard SPM5 PET template. The color bar represents Z-values. The left side of each picture is the right side of the brain.

Table 1

Significant differences in cerebral blood flow (CBF), cerebral blood volume (CBV), mean transit time (MTT) and time-to-peak (TTP) at interictal stage

	Brain area	MNI coordinates (x y z)	Cluster-size	Z-value
CBF (ml/100g/min)				
Increased				
Migraine (55.8 [9.2]) vs. controls (45.1 [6.1])	L Medial frontal gyrus	−6 28 38	48	4.21
MA (55.8 [10.7]) vs. controls (44.1 [6.3])	L Medial frontal gyrus	−8 26 40	34	3.82
MO (62.8 [9.0]) vs. controls (50.1 [6.9])	L Medial frontal gyrus	−6 28 38	20	3.76
MO (41.1 [4.3]) vs. controls (33.9 [8.5])	R Inferior temporal gyrus	32 2 −52	26	3.70
Decreased				
MA (31.7 [4.1]) vs. controls (34.7 [8.2])	R Inferior temporal gyrus	36 0 −50	49	4.47
MA (43.4 [3.9]) vs. controls (45.8 [9.5])	L Postcentral gyrus	−48 −24 32	24	3.41
MO (49.9 [7.8]) vs. controls (61.9 [12.1])	L Inferior frontal gyrus	−54 20 32	26	3.82
CBV (ml/100g)				
Increased				
MO (4.1 [0.9]) vs. controls (3.9 [1.0])	R Middle temporal gyrus	48 −16 −12	26	3.51
MO (2.3 [0.5]) vs. controls (2.3 [0.7])	R Inferior temporal gyrus	38 −2 −48	30	3.41
MO (2.4 [0.6]) vs. controls (2.2 [0.4])	R Inferior temporal gyrus	58 −30 −22	22	3.34
No decreases				
MTT (s)				
No increases or decreases				
TTP (s)				
No increases or decreases				

MA=migraine with aura, MO=migraine without aura, MNI=Montreal Neurological Institute; p<0.001, uncorrected, cluster extent threshold of 20 voxels; between brackets mean [SD] CBF, CBV, MTT and TTP values of corresponding clusters across subjects per group

Table 2

Significant differences in cerebral blood flow (CBF), cerebral blood volume (CBV), mean transit time (MTT) and time-to-peak (TTP) at interictal stage between high (HF, >2 attacks, n=12) and low (LF, ≤2 attacks per month, n=13) frequency migraine and controls (n=16)

	Brain area	MNI coordinates (x y z)	Cluster - size	Z-value
CBF (ml/100g/min)				
Increased				
HF (64.9 [8.9]) vs. controls (50.8 [7.2])	L Medial frontal gyrus	−6 26 38	88	4.71
HF (56.5 [4.8]) vs. LF (47.4 [4.9])	L Postcentral gyrus	−38 −26 48	54	4.39
HF (67.0 [9.2]) vs. LF (56.5 [6.3])	L Precentral gyrus	−58 0 6	27	4.05
HF (82.0 [8.5]) vs. LF (64.7 [9.4])	L Medial frontal gyrus	−4 28 32	52	4.04
HF (72.0 [10.0]) vs. LF (59.3 [6.9])	R Putamen	38 −8 −2	65	3.92
HF (65.9 [7.0]) vs. LF (54.9 [7.9]	L Postcentral gyrus	−62 −10 20	23	3.83
HF (48.3 [5.3]) vs. LF (38.2 [6.6])	L Medial frontal gyrus	−32 18 44	30	3.82
HF (45.2 [6.9]) vs. LF (36.4 [4.4])	R Inferior parietal lobule	44 −28 24	103	3.81
HF (87.5 [14.4]) vs. LF (66.4 [8.3])	R Cingulate cortex	10 38 4	52	3.78
HF (67.6 [9.7]) vs. LF (57.3 [5.0])	R Superior frontal gyrus	8 −28 56	25	3.72
HF (58.1 [8.0]) vs. LF (46.6 [4.3])	R Middle frontal gyrus	32 46 26	43	3.58
HF (87.1 [10.0]) vs. LF (70.0 [11.0])	R Superior frontal gyrus	18 −62 16	30	3.52
HF (53.9 [12.5]) vs. LF (40.0 [6.9])	L Medial frontal gyrus	−28 34 26	29	3.40
HF (58.5 [10.4]) vs. LF (50.0 [5.5])	R Inferior frontal gyrus	50 50 2	28	3.39
Decreased				
LF (56.0 [6.5]) vs. controls (67.9 [13.3])	L Medial frontal gyrus	−54 20 32	30	3.55
CBV (ml/100g), MTT (s), TTP (s)				
No increases or decreases				

MNI=Montreal Neurological Institute; p<0.001, uncorrected, cluster extent threshold of 20 voxels; between brackets mean [SD] CBF, CBV, MTT and TTP values of corresponding clusters across subjects per group

Table 3

Significant differences in cerebral blood flow (CBF), cerebral blood volume (CBV), mean transit time (MTT) and time-to-peak (TTP) at interictal stage between long (LH, >28 years, n=13) and short (SH, ≤28 years of headache, n=12) migraine history and controls (n=16)

	Brain area	MNI coordinates (x y z)	Cluster-size	Z-value
CBF (ml/100g/min)				
Increased				
SH (71.2 [11.6]) vs. controls (53.8 [7.9])	L Medial frontal gyrus	−6 26 38	45	4.33
LH (45.0 [6.6]) vs. SH (37.5 [5.9])	L Medial frontal gyrus	−34 18 44	20	3.76
LH (53.7 [10.6]) vs. SH (42.2 [7.3])	L Medial frontal gyrus	−30 32 30	30	3.52
SH (63.0 [7.5]) vs. LH (48.0 [3.8])	R Inferior parietal lobule	58 −38 26	28	4.09
No decreases				
CBV (ml/100g)				
Increased				
SH (2.5 [0.6]) vs. controls (1.9 [0.4])	R Cerebellum	22 −52 −70	138	4.09
SH (4.0 [0.9]) vs. controls (3.5 [0.7])	L Occipital gyrus	−30 −94 −14	52	3.81
SH (4.7 [1.1]) vs. controls (4.1 [0.8])	L Medial frontal gyrus	−4 28 38	21	3.61
SH (3.8 [0.8]) vs. controls (3.2 [0.6])	L Cerebellum	−20 −46 −66	32	3.46
SH (2.4 [0.6]) vs. controls (2.0 [[0.4])	R Inferior temporal gyrus	54 −30 −32	28	3.41
SH (3.3 [1.0]) vs. LH (2.2 [0.7])	R Cerebellum	24 −52 −70	77	3.68
SH (4.7 [1.0]) vs. LH (3.3 [0.7])	R Inferior parietal lobule	64 −40 24	25	3.63
SH (3.8 [0.8]) vs. LH (2.8 [0.7])	L Superior frontal gyrus	−22 12 68	26	3.53
No decreases				
MTT (s)				
Increased				
SH (2.5 [0.7]) vs. controls (2.3 [0.5])	R Cerebellum	20 −54 −68	186	3.80
SH (3.3 [0.8]) vs. controls (3.5 [0.4])	L Inferior parietal lobule	−50 −52 48	39	3.30
SH (3.9 [1.0]) vs. controls (4.0 [0.6])	R Inferior frontal gyrus	50 12 6	22	3.23
SH (2.8 [0.8]) vs. LH (2.2 [0.8])	R Cerebellum	26 −56 −70	51	3.46
SH (4.2 [0.7]) vs. LH (4.0 [0.7])	R Medial frontal gyrus	38 22 32	21	3.32
No decreases				
TTP (s)				
No increases or decreases				

MNI=Montreal Neurological Institute; p<0.001, uncorrected, cluster extent threshold of 20 voxels; between brackets mean [SD] CBF, CBV, MTT and TTP values of corresponding clusters across subjects per group